International Journal of Pharmaceutics: X 8 (2024) 100267

Contents lists available at ScienceDirect

International Journal of Pharmaceutics: X

journal homepage: www.sciencedirect.com/journal/international-journal-of-pharmaceutics-x

Development and optimization of the Glabridin-loaded dissolving microneedle for enhanced treatment of keloid

Juan Guo [a,1], Zhongtang Chen [a,1], Rong Huang [a], Dandan Tang [a], Yuhuan Wang [a,b], Pan Song [c], Liangyu Mei [a], Shuguang Hou [a], Wei Peng [a,**], Lisha He [a,**], Qiang Ren [a,b,*]

[a] State Key Laboratory of Southwestern Chinese Medicine Resources, School of Pharmacy, School of Clinical Medicine, Chengdu University of Traditional Chinese Medicine, Chengdu 611137, PR China
[b] Hospital of Chengdu University of Traditional Chinese Medicine, Chengdu University of Traditional Chinese Medicine, Chengdu 610075, PR China
[c] Chengdu Integrated TCM & Western Medicine Hospital, Chengdu 610041, PR China

ARTICLE INFO

Keywords:
Dissolving microneedle
Glabridin
Keloid
Transdermal absorption
PI3K/Akt signaling
TGF-β1/α-SMA

ABSTRACT

Glabridin (Gla) has been reported to have significant effects in scar treatment, and however, the water insolubility of Gla leads to its poor transdermal absorption ability, which affects its bioactivities. Therefore, we attempted to prepare the Gla dissolving microneedles (Gla-MN) to improve the absorbtion of Gla. After investigation of the 3 factors including the needle tip matrix concentration, the prescription concentration of backing material, and the dissolution method of Gla, we finally determined the process parameters of 10% hyaluronic acid (HA) as the needle tip and 5% polyvinyl alcohol (PVA) as the backing, according to which the Gla-MN was prepared with the good characteristics of high hardness, complete appearance and good in vitro dissolution ability. We then loaded Gla onto the microneedles and measured that the average drug loading of Gla-MN was 2.26 ± 0.11 μg/mg and the cumulative transdermal release of Gla-MN was up to 76.9% after 24 h. In addition, Gla-MN had good skin penetration properties, with Gla-MN penetrating at least 4 to 5 layers of parafilm. And the skin basically could return to normal after 4 h of piercing. Importantly, our results showed that Gla-MN had higher transdermal delivery and therapeutic effects against keloid than that of Gla at the same dosage.

1. Introduction

Keloid is a benign fibroproliferative scar due to excessive proliferation of fibrous connective tissue commonly caused by traumatic wounds or skin infections. Keloid is characteristized by continuous proliferation of fibroblasts and invasive growth of adjacent tissues, as well as excessive secretion of extracellular matrix (Chen et al., 2024; Yan et al., 2023). It generally exists in the deep dermis and is difficult to be removed, often leading to skin deformities and impaired skin function. Importantly, it seriously affects the appearance of the body, causing a great psychological burden on keloid patients (Limandjaja et al., 2020; Luan et al., 2016). Although many treatment methods for keloids coulbe be used, including surgery and drug treatements, the overall therapeutic effects of these treatments are unsatisfactory and regretful due to the poor therapeutic effect, severe side-effects and highly recurrence rate, etc. (Ghadiri et al., 2022; Jiang et al., 2020). For the keloid treatment, the majority of the population would like to choose topical medication and local injection therapy. However, local external drugs are difficult to reach the dermis due to the obstruction of the skin barrier, thus exerting their effects. Additionally, topical injection therapy makes it difficult to carry the drug to a specified depth of skin, resuliting in uneven distribution of drugs within the scar and unsatisfactory anti scar effects (Ward et al., 2019). Therefore, it's necessary to discovery more active substances and devlop more feasible drug delivery systems for treatment or prevention of keloid. Increasing studies have suggested that natural products have good biocompatibility with human beings due to the coevolution of organisms on Earth, and have been used to treat various diseases for thousands of years (Peng et al., 2024).

Glabridin (Gla) is a flavonoid compound with a wide spectrum bioactivities extracted from the traditional Chinese medicine of licorice. In

* Corresponding author at: State Key Laboratory of Southwestern Chinese Medicine Resources, School of Pharmacy, School of Clinical Medicine, Chengdu University of Traditional Chinese Medicine, Chengdu 611137, PR China.
** Corresponding authors.
E-mail addresses: pengwei@cdutcm.edu.cn (W. Peng), helisha@cdutcm.edu.cn (L. He), renqiang@cdutcm.edu.cn (Q. Ren).
[1] Contributed equally to this work.

https://doi.org/10.1016/j.ijpx.2024.100267
Received 28 April 2024; Received in revised form 22 June 2024; Accepted 29 June 2024
Available online 1 July 2024

our previous research, Gla has been confirmed to have significant effects in scar treatment. Gla could inhibit HKF cell proliferation by inducing cell apoptosis and could also reduce collagen production in HKF cells. The further molecular mechanism studies have revealed that the anti-scar effects of Gla is closely related to regulation of PI3K/Akt and TGFβ1/SMAD pathway (Zhang et al., 2022b). However, the water insolubility of Gla leads to its poor transdermal absorption ability, which affects its bioactivities (Hespeler et al., 2019; Simmler et al., 2013). Therefore, we attempted to find a suitable dosage form for Gla, and finally found that microneedle might be a feasible drug administration system for increasing the absorbtion of Gla.

The specification of microneedles is generally 10-2000 μm in height and 10-50 μm in diameter. It generally cause temporary physical damage to the stratum corneum of the skin through micron-sized needle tips, creating microporous channels through which drugs are directly transported to the epidermis or upper dermis (Jamaledin et al., 2020; Zhang et al., 2022a). Microneedles can not only maintain the advantages of traditional transdermal drug delivery systems, but also overcome the problems of insufficient permeability and low drug delivery efficiency, and have been widely used in transdermal drug delivery systems. Due to the fact that microneedle administration generally does not cause pain, it greatly improves patient compliance (Kim et al., 2012; Knopf-Marques et al., 2016; Zhang et al., 2021). Therefore, in this study, we developed the Gla-loaded dissolving microneedles to increase the treatment of Gla against keloid. As the most of our knowledge, this is the first report regarding Gla-loaded dissolving microneedles, and our present work provides a new cadidate way for the treatment of keloid.

2. Materials and methods

2.1. Materials

Gla (purity over 98%) was purchased from Chengdu Maidesheng Technology (Cat. No. RP201203, Chengdu, China); Hyaluronic acid (99%) was purchased from Shanghai Yihui Biotechnology (Cat. No. RH335738, Shanghai, China); Poloxamer 188 was purchased from Xi'an Jinxiang Pharmaceutical Accessories (Cat. No. GND31621B, Xi'an, China); Polyvinyl alcohol 17–99 was purchased from Chengdu Kelong Chemical Reagent Factory (Chengdu, China); Phosphate buffer solution (PBS) was purchased from Shanghai Chuangsai Technology (Shanghai, China); 4% paraformaldehyde fixative from biosharp (Cat. No. 23179318, Shanghai, China); Sodium pentobarbital is purchased from Sigma (Cat. No. 20190614, Shanghai, China); Primary antibodies of Akt, phosphorylation (p)-Akt, Bax, Bcl-2, cleaved (c)-Capease-3, TGF-β1, PI3K, p-PI3K,α-SMA and β-actin were purchased from Abclonal (Wuhan, China). Microneedle mold was purchased from the Precision Technology (Dongguan, China).

2.2. Animals

New Zealand rabbit (1.8–2.5 kg) was purchased from the Chengdu Dashuo Experimental Animal (Chengdu, China), and were kept under constant conditions (temperature 25 ± 1 °C). Rabbits were randomly divided into four groups: normal keloid group (Control), Gla group, Blank-MN group and Gla-MN group ($n = 5$) (Hong et al., 2018; Zhong et al., 2024). Briefly, rabbits were anesthetized by intravenous injection of pentobarbital sodium (30 mg/kg, iv.), and subequently the cartilage in rabbit ears was exposed with a hole punch. Each rabbit had six lesions. After the wound is covered with iodophor, the scab is removed after seven days, causing a secondary wound, and the wound is closed with a sterile bandage. Sterile dressing is removed at the end of the 3th week. The Contorl rabbits were administered with normal saline twice a day, the Gal rabbits were administered with Gla solution twice a day, and the Blank-MN and Gla-MN rabbits were administered with blank microneedles and Gla-loaded microneedles, respectively, and the needle was inserted into the scar. After 12 days' treatment, the rabbits were sacrificed by intravenous injection of pentobarbital sodium (100 mg/kg, iv.). Then, each scar tissue was collected, and 4% of the paraformaldehyde was used to fixed the scar tissues for histopathological examinations with H&E staining and masson staining, and the remaining samples were used for further biochemical examinations. All the animal protocols were approved by the Institutional Ethics Committee of Chengdu University of TCM (approval no. 2023208).

2.3. Preparation of Gla-MNs

Glabridin-loaded dissolving microneedle (Gla-MN) were prepared using a two-step casting method as shown in the flowchart (Fig. 1). Firstly, Gla, poloxamer 188 and HA were placed in a mortar, and the mixture was ground until Gla was completely dissolved to obtain the matrix solution constituting the tip of the microneedles. The matrix solution was then casted onto the polydimethylsiloxane (PDMS) microneedle mold, and subsequently placed in a vacuum dryer and filled three times for five minutes every times under negative pressure to fill the mold cavities with the tip matrix solution. The excess tip matrix solution was gently scraped off. Next, the PVA solution was added to the mold as the backing membrane of the microneedle. Finally, the prepared microneedles were dried with constant temperature at 40 °C for 24 h to form the final product of the Gla-MNs (Cheng et al., 2020), and the prepared Gla-MNs were stored in a desiccator for the following experiments.

2.4. Formulation optimization of PVA and HA

Hyaluronic acid (HA) is one of the commonly used microneedle tip matrix materials which has biodegradability, diversity, biocompatibility and excellent non-immunogenicity. Low molecular weight HA has good formability, strong hardness, and good properties for the preparation of needle tip (Knopf-Marques et al., 2016). Similarly, as a commonly used backing material, polyvinyl alcohol (PVA) has the characteristics of good toughness, good texture, and close fit with the skin. Therefore, we chose HA as the needle tip substrate and PVA as the backing material (Xing et al., 2023). Furthermore, three concentrations of HA (5%, 10% and 15%) were tested for optimization of the tip material, three concentrations of PVA 17–99 (5%, 10% and 15%) were tested for optimization of the backing material. Gla is difficult to dissolved in HA solution, so a certain amount of solubilizer is added. We chose poloxamer 188 as the solubilizer, and we mixed Gla with poloxamer 188 and HA at the ratio of 5:1, 3:1, 2:1 and 1:1 to observe their dissolution.

2.5. Morphological characterization

A macro camera, a Baisite 500× magnifier and a scanning electron microscope were used to observe whether the backing layer of the microneedle patch was flat, the individual needle body and the arrangement of the microneedle array.

2.6. Microneedles solubility test in vitro

Pre-treated mouse skins were incubated in PBS (pH 7.4) for 1 h, and then the stratum corneum side of the skin was dried and placed on a paper towel impregnated with PBS (pH 7.4) solution, and the isolated skin was placed at 37 °C to simulate the in vivo environment. The microneedle was then inserted into the mouse skin, removed after a period of time, and the morphological changes of the microneedle were observed using a Baisite magnifying microscope.

2.7. Mechanical performance tests

The mechanical properties of the microneedles were assessed by a texturing instrument. The microneedles, cut the excess uneven backing material, were placed on the horizontal platform of the texturing

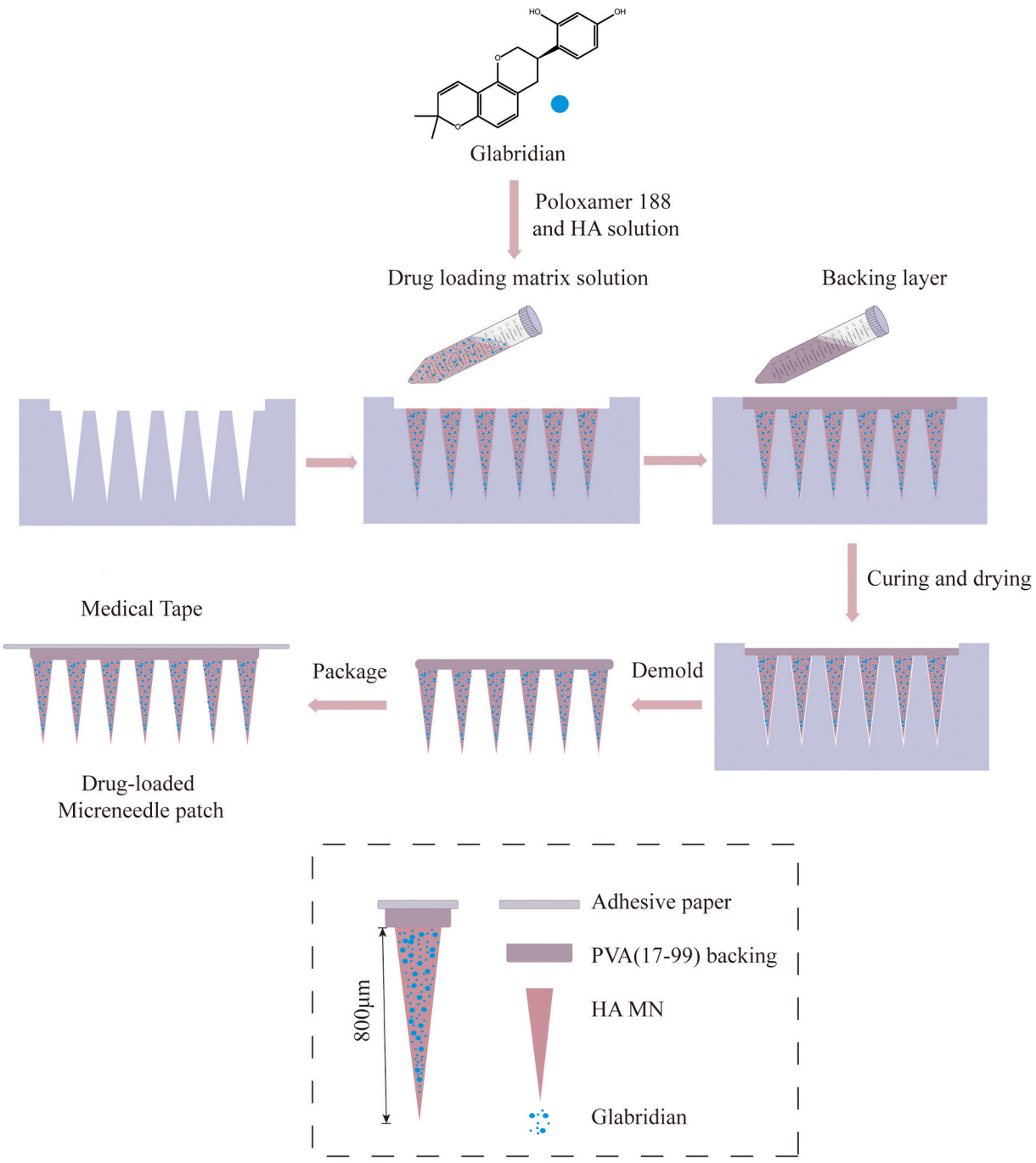

Fig. 1. Preparation of Gla-MN. The dashed frame shows the composition of the Gla-MNs.

instrument with the tip facing upwards, and the P5 probe was used to move vertically downwards at a speed of 5 mm/min to record the forces on the microneedles throughout the testing process and to plot the force/needle - displacement curves.

2.8. Determination of microneedle drug loading by HPLC

The Gemini C_{18} (250 × 4.6 mm, 3 μm) liquid chromatography column was selected with pure water as mobile phase A and acetonitrile as mobile phase B. The method of isodegree elution was adopted at the flow rate of 1.0 mL/min. The sample size was 10 μL, the column temperature was 30 °C, and the detection wavelength was 282 nm (Viswanathan and Mukne, 2016). Precision weighing 4 mg of Gla reference agent, using 75% methanol to dissolve to 5 mL volumetric bottle scale line, shake well to obtain a mass concentration of 0.8 mg/mL Gla reference agent reserve solution. The prepared Gla-MNs were dissolved in 5 mL methanol solution (75%) and then filtered with 0.22 μm microporous filter membrane after ultrasound to obtain the testing sample solution (Wei et al., 2015). Then, methodological investigation was carried out to evaluate the rationality and accuracy of the Gla-MN preparation process.

2.9. Skin puncture property and recovery assays

Mice were anesthetized by intravenous injection of pentobarbital sodium (45 mg/kg, iv.) and then the mice were sacrificed by decapitation. Then, the skins of abdomen and dorsal backs of the mice was seprated and the subcutaneous fat and fascia were removed, and the

prepared Gla-MN was stabbed into the skin samples, and then the pricked part was stained with Trypan blue. The stained solution remained on the skin for 30 min and then washed with PBS (Wang et al., 2022). Subsequently, the skin was fixed with 4% paraformaldehyde for 24 h, then dehydrated with ethanol and embedded in paraffin, and was cut into 5 μm slices. Finally, the hematoxylin and eosin (H&E) staining was carried out and photographed under an optical microscope.

Furthermore, we also evaluated the safety of Gla-MNs on the skin. Briefly, the Gla-MNs were placed on the inner skin of rabbit ears and kept pressing with a certain force for 2 min. Draize method was used to evaluate the irritation on the skin according to the degree of erythema, eschar and edema before and after the application of Gla-MNs (Srivastava et al., 2022). The whole process of rabbit ear skin healing was recorded with camera, and the sites without microneedles treatments were used as control.

2.10. Parafilm membrane insertion assay

To visualise the depth of insertion of the microneedle into the skin, 8 layers of Parafilm™ (approximately 1 mm) were stacked and placed on the foam. After inserting the microneedle into the Parafilm™ membrane, pressure was applied for approximately 30 s. Then the microneedle was removed, and the number of layers of the membrane punctured by the microneedle was recorded.

2.11. In vitro percutaneous permeability test

In vitro transdermal study of mouse skin was carried out using Franz diffusion cell (Sabbagh et al., 2023; Zhong et al., 2024). Briefly, Gla-MN was inserted into the skin without subcutaneous fat, and the skin was fixed and dipped into a diffusion tank (Ronnander et al., 2018). The extracted liquid was then filtered by a 0.22 μm microporous filter membrane, and the drug concentration was detected by HPLC.

2.12. Histopathological examinations

H&E and Masson staining were used to observe the characteristics of fiber hyperplasia and inflammatory infiltration. Masson staining was mainly used to observe the number and arrangement of collagen fibers in scar tissue (Ahn et al., 2023). A field of view was randomly selected for each sample and recorded, and the relative fiber tissue expression was calculated using Image J software.

2.13. Western blot

Total proteins of the scar tissues were extracted using the Protein Purification & Isolation kits (Cat. No. 78510, Thermo Scientific™, Shanghai, China), and then the protein was isolated by electrophoresis with sodium dodecyl sulfate polyacrylamide gel (SDS-PAGE) and transferred to PVDF membrane. The expression levels of Bax, Bcl-2, TGF-β1, C-Capease-3, p-Akt, p-PI3K, Akt, PI3K and α-SMA were detected with corresponding antibodies, and β-actin and β-Tubulin were used as internal reference proteins to regulate the amounts of samples (Chen et al., 2021; Fang et al., 2016; Zhang et al., 2017b; Zhang et al., 2020).

2.14. Statistical analysis

All the data were statistically analyzed by GraphPad Prism 9 software (GraphPad Software, LLC. San Diego, CA, USA), and the results were expressed as mean ± SD. One-way analysis of variance (ANOVA) was used to determine the significance of the results, and $P < 0.05$ was considered statistically significant.

3. Results and discussion

3.1. Optimal parameters for preparation of Gla-MNs

In our previous study, we have reported that Gla possessed a therapeutic role against keloid (Zhang et al., 2022b). However, the poor solubility and low bioavailability of this natural compound seriously limit the application of Gla in the treatment of dermal diseases (Lu et al., 2024; Zhang et al., 2017a). Microneedle (MN) patch is an effective transdermal drug delivery system (TDDS) with the ability to overcome the stratum corneum barrier, which seems as a feasible way for enhancing the bioavailability of Gla (Yang et al., 2021). Therefore, in our present study, we developed the Gla-loaded dissolving microneedles in order to increase the curative effect of Gla against keloid.

As illustrated in Fig. 2 A, when the concentration of the backing PVA is 15%, the solution is excessively viscous, the bubbles can not be completely eliminated when vacuuming, the hardness is excessively high after curing, and the shape of the backing formed cannot meet the requisite specifications. As the concentration of PVA decreases, the flexibility of the backing material improves. The formability of microneedles was used as an indicator to select 5% PVA as the backing.

Microneedles with tip concentrations of 5%, 10%, and 15% HA were prepared with 5% PVA as the backing, as shown in Fig. 2 B, and the microneedle patch had a square shape, measuring 15 mm × 15 mm. As illustrated in Fig. 2 C—D, it can be observed that the microneedles prepared with 5% HA exhibited a bent tip and a small amount of needle breakage, accompanied by a concave and uneven needle column. As the HA concentration increased, the tip of the microneedle exhibited better molding and greater sharpness. The microneedle patch with tip concentration of 10% or 15% exhibited transparency and uniformity in colour, with equal spacing between needles, a flat bottom layer, no obvious air bubbles, and the needles were neatly arranged to form a 20 × 20 microneedle array. The shape of the needle body was basically complete and consistent, exhibiting a conical shape, a smooth surface, sharp tips, and the absence of cavities or fractures.

Subsequently, the in vitro dissolution of the tips was recorded at 5, 25, and 45 min for the three concentrations, as shown in Fig. 2 E. After 45 min, the tip of the 5% HA preparation was completely dissolved, and the dissolution deteriorated as the concentration was increased. In contrast, the tip of the 15% HA preparation was still mostly undissolved. Furthermore, the mechanical properties of the microneedle tip were evaluated (Fig. 2 F). Ning et al. reported that the minimum force required to penetrate the single MN was 0.058 N per needle (Ning et al., 2020). Our results showed that the force per needle tip for 5% HA, 10% HA and 15% HA concentrations was 0.021 N, 0.062 N and 0.042 N, respectively, when the needle length was compressed to half the length. This suggested that the tips of needles prepared with 5% HA and 15% HA may not be able to penetrate the skin. From the whole curve analysis, the force-displacement curves of 15% HA and 10% HA were similar, which may be due to the fact that the concentration of 15% HA was too high and the concentration filled into the needle tip during the vacuum filling process could not reach the actual concentration. A summary of the aforementioned experiments revealed that a concentration of 10% HA at the tip of the microneedle and 5% at the back of the needle was optimal for the preparation of microneedles.

Furthermore, since Gla is insoluble in water, a solubilizer (poloxamer 188) was employed to dissolve Gla. During the experiment, it was found that 5 mg of Gla and 2.5 mg of poloxamer 188 could completely dissolve the Gla in 1 mL of the tip matrix, which was lower than the case where 2.5 mg of Gla could not completely dissolve. Consequently, a 2:1 mass ratio of Gla and poloxamer 188, dissolved in 1 mL of 10% hyaluronic acid (HA) solution, was selected as the drug-containing tip matrix.

3.2. Results of the drug loading in microneedle determination

The prepared Gla-MN was dissolved ultrasonic in 75% methanol.

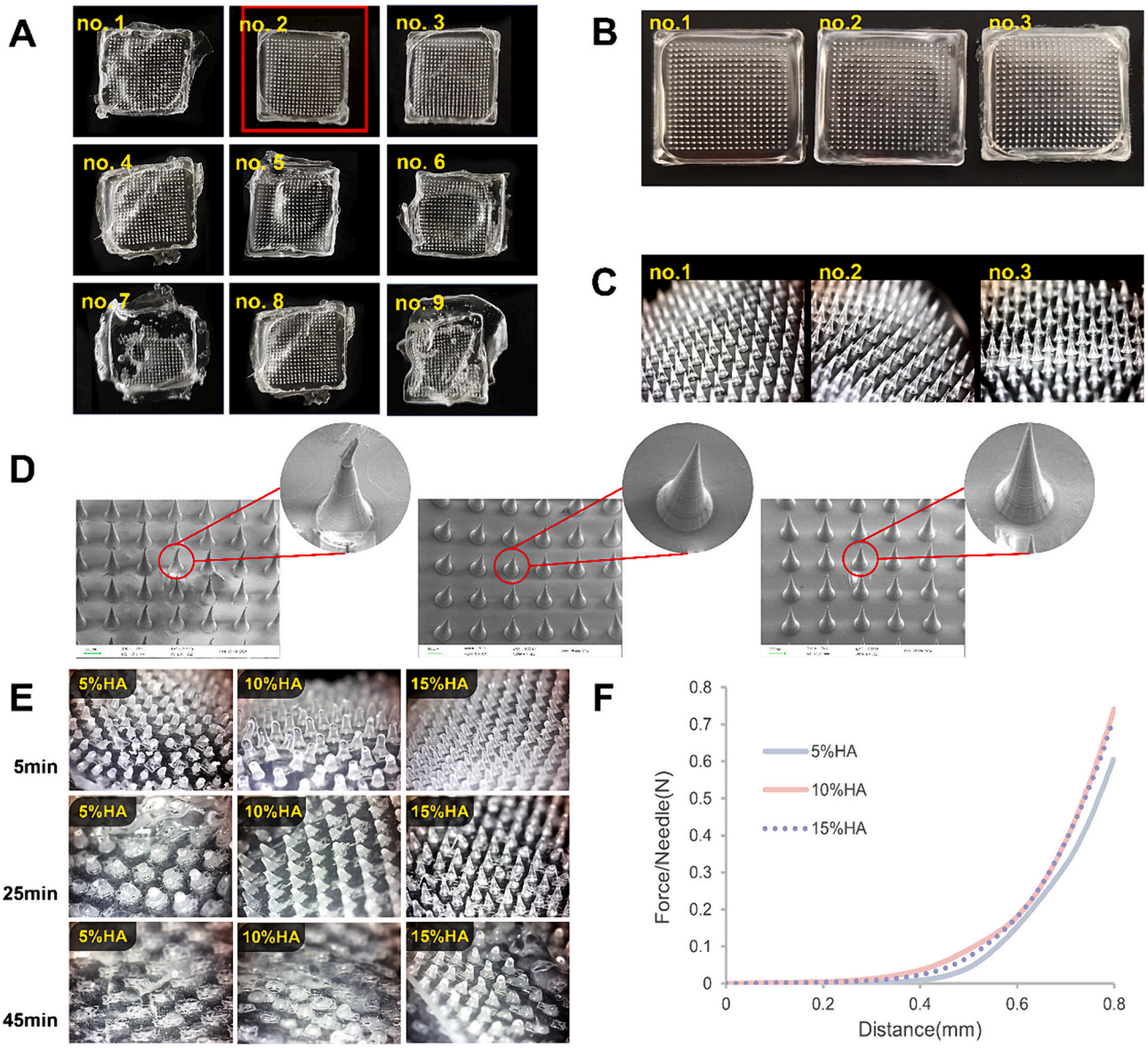

Fig. 2. Processing optimization of Gla-MN. (A) Appearance of the MN using different processing parameters(no.1-no.3 shows the morphology of microneedles with 5%, 10%, and 15% HA solution as the tip and 5% polyvinyl alcohol as the backing, respectively; no.4-no.6 shows the morphology of microneedles with 5%, 10%, and 15% HA solution as the tip and 10% polyvinyl alcohol as the backing, respectively; no.7-no.9 shows the morphology of microneedles with 5%, 10%, and 15% HA solution as the tip and 15% polyvinyl alcohol as the backing, respectively). (B)-(C) Frontal and tip appearance of microneedle prepared with different concentrations of HA. No.1, no.2 and no.3 are microneedles prepared with 5%, 10% and 15% HA, respectively. (D) SEM images of the Gla-MN. (E) Dissolution of microneedle tips prepared with different concentrations of HA (5%, 10%, 15%) after 5, 25 and 45 min respectively. (F) Mechanical properties of needle tips prepared with different concentrations of HA (5%, 10%, 15%).

Subsequently, the Gla contents in each part of the microneedle was determined by HPLC, and the results showed Gla contents in each part of the microneedle was 44.73, 43.98, 45.13, 48.05, 42.57, 42.15 μg, with an average drug content per milligrams at 2.24 μg/mg, 2.18 μg/mg, 2.22 μg/mg, 2.37 μg/mg, 2.25 μg/mg, 2.28 μg/mg; the average weight per attached drug of Gla-MN was (44 ± 2) μg and RSD was 4.75%, the average loaded drug content was 2.26 μg/mg, and the RSD was 0.06% (Fig. S1 & Tab. S1).

3.3. Skin and parafilm puncture performance and the healing of the skin after Gla-MN penetration

A good skin penetration ability for the microneedle is a guarantee for overcoming the stratum corneum barrier (Sartawi et al., 2022; Zhan et al., 2023). In our present investigation, the skin penetration ability of the prepared Gla-MN is determined using mouse skin puncture test with trypan blue staining. Trypan blue is a cellular reactive dye that is commonly used to detect cell membrane integrity and cell survival. Normal living cells with an intact cell membrane structure are able to repel trypan blue and prevent it from entering the cell. In contrast, inactive or incomplete cells with increased cell membrane permeability can be stained blue by trypan blue(Zhang et al., 2022b). The results of microneedle puncture and staining of mouse skin with trypan blue solution are shown in Fig. 3 A. The left figure represented the skin condition before staining, and the right figure showed the skin condition after dyeing trypan blue, and it can be seen that the pinhole parts in the mouse skin are stained blue, indicating the testing Gla-MN has a good skin penetration ability.

The insertion depth of the microneedle was approximately 100 μm, as determined by H&E staining (Fig. 3 B). In fact, the actural insertion

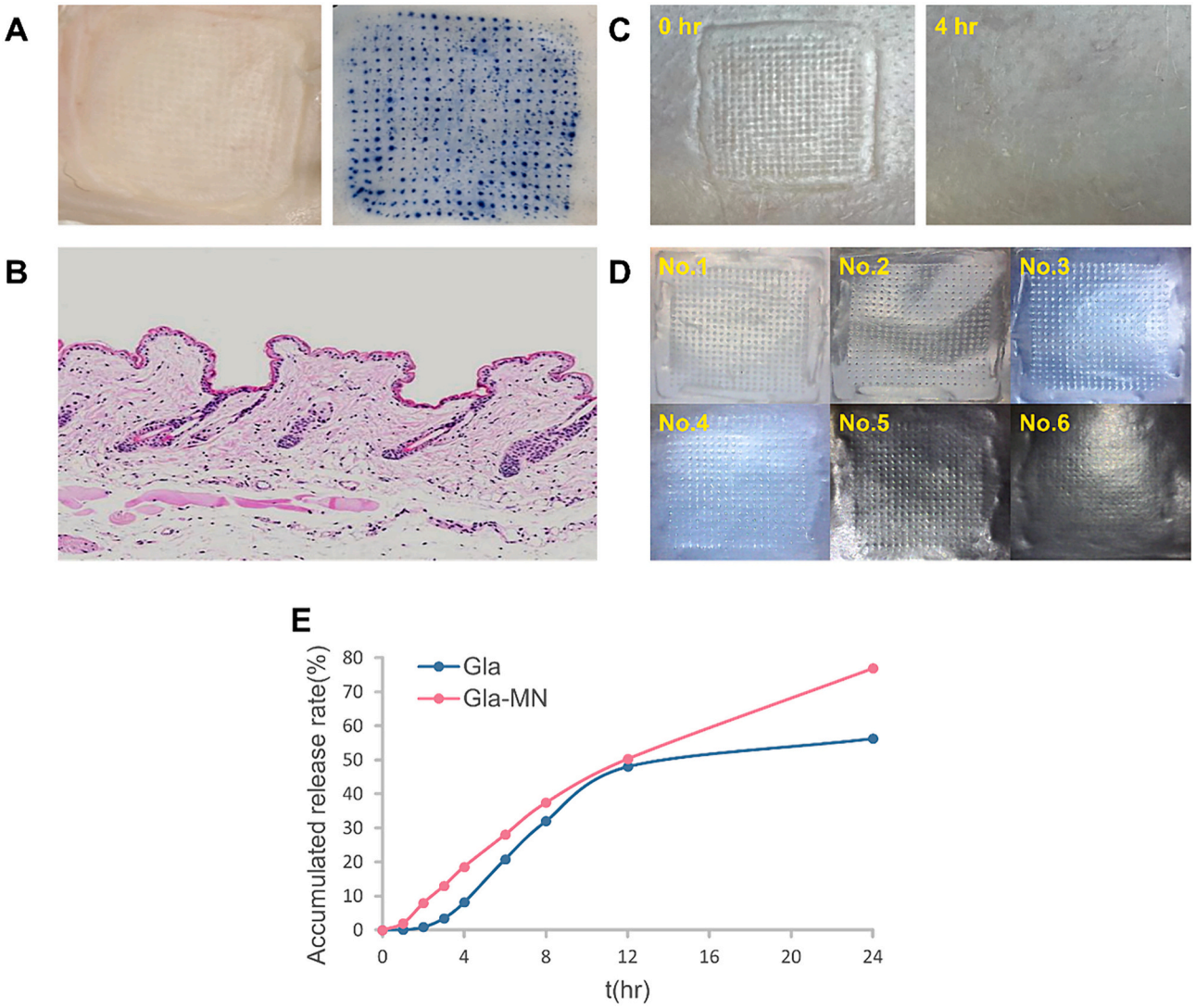

Fig. 3. Skin puncture performance and accumulated release rate of Gla-MN. (A) Skin puncture performance of Gla-MN without or with trypan blue staining, respectively. (B) H&E straining of the skin after penetration of Gla-MN. (C) The healing of the skin after Gla-MN penetration. (D) Parafilm membrane puncture test (No.1 ~ No.6 are the first to sixth parafilm layers after applying Gla-MN). (E) Accumulated release rate of Gla-MN. (For interpretation of the references to colour in this figure legend, the reader is referred to the web version of this article.)

depth of the microneedles was over than 100 μm, which can completely overcome the stratum corneum barrier of the skin. However, the determined piercing depth was only 100 μm by the pathological examination with H&E staining, and this results might be not very suitable for determine the real piercing depth of the microneelds. Firstly, due to the well-developed subcutaneous muscle groups in mice, the skin will recoil after the microneedle is inserted into the skin; Secondly, the skin will gradually heal during the sampling process and will be deformed during the processing of the samples, causing the measured data to deviate from the actual data. Therefore, we also determined the piercing ability of the Gla-MNs with the Parafilm Membrane Insertion Assay.

Parafilm is a commonly used material in human skin modelling due to its elasticity, which resembles the human skin, and its insertion resistance. Therefore, Parafilm insertion experiment was included in the experiment. As illustrated in Fig. 3 D, the microneedle was capable of puncturing the first four layers of Parafilm. Based on the imprint of the sixth layer, it can be observed that the tip of the middle of the microneedle was able to pierce the Parafilm to the sixth layer, whereas the tip of the edge of the microneedle patch was only able to leave an imprint on the fifth layer. This calculation indicates that the depth of microneedle penetration is approximately 500 to 625 μm. The stratum corneum is approximately 15–20 μm, and the epidermis is about 150–200 μm, and the dermis is about 1–3 mm. Consequently, it can be theoretically assumed that all microneedles can successfully penetrate the dermis to form micro-channels, thereby accelerating the delivery of drugs. Furthermore, four hours after the in vivo puncture of Gla-MN, the skin exhibited complete healing without any evidence of redness, swelling, or inflammation (Fig. 3 C).

3.4. Accumulated release rate of Gla-MN

The cumulative release rate of Gla-MN in the skin reached 76.9% at 24 h, and, compared with Gla solution, the drug delivery was significantly increased (Fig. 3 E).

3.5. Anti-scar hyperplasia effects of the Gla-MN

In our present study, we compared the anti-scar hyperplasia effects between Gla and Gla-MN. After treatment with drugs for twelve days, anti-scar effects of the Gla and Gla-MN were evaluated, and the scar hyperplasia in each group is shown in Fig. 4. As can be seen from the Fig. 4, although both Gla and Gla-MN have good anti-scar hyperplasia

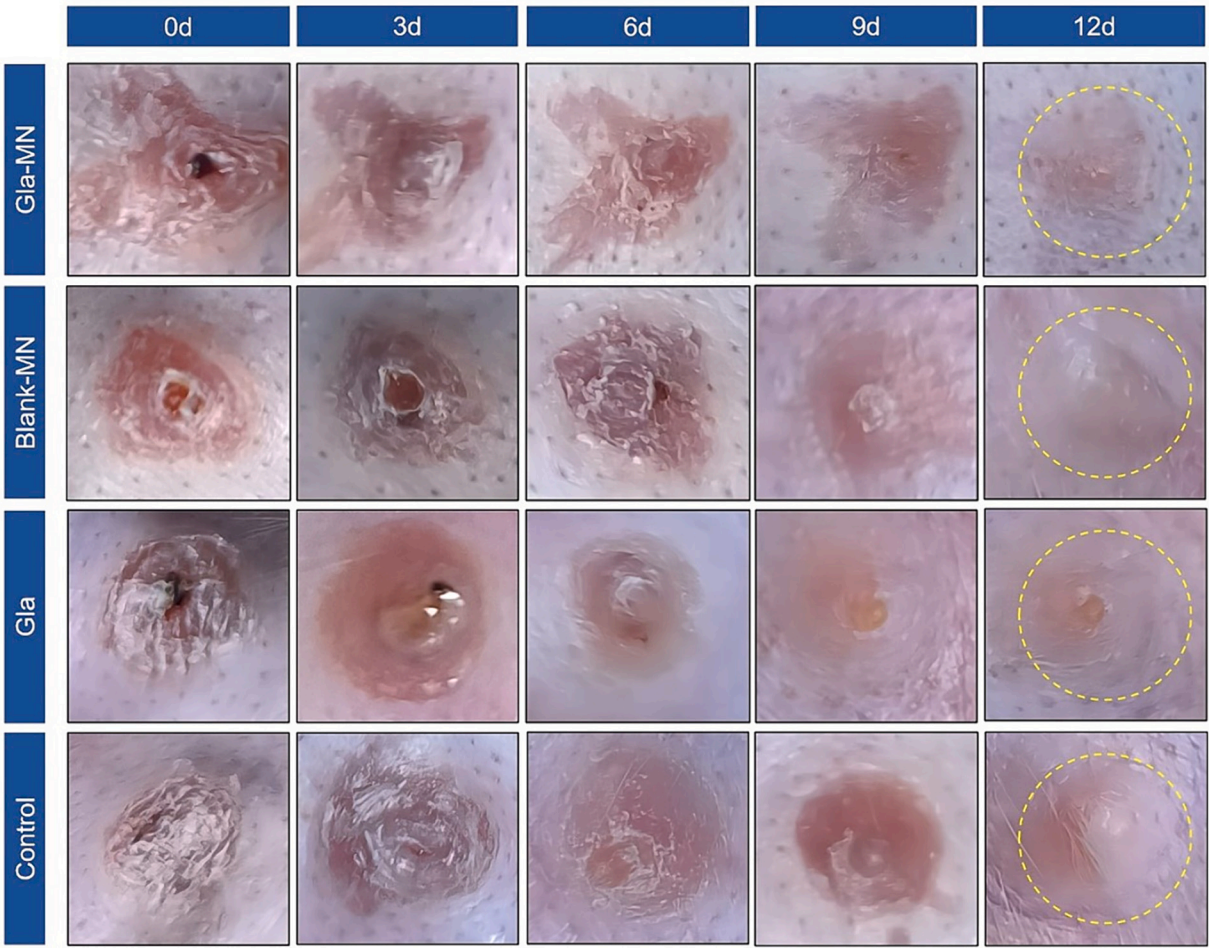

Fig. 4. Images of gross examination of Gla and Gla-MN during 12 days.

effects compared with the rabbits in Control group, the scar thickness in the Gla-MN treated rabbit ear was obviously lower than that of Gla group. Additionlly, our results also indicated that the blank MN had no obvious treatment effect on scar hyperplasia of rabbit ear compared to the Control rabbit (Fig. 4), indicating that the blank delivery system carrier had no effect on the scar hyperplasia. Furthmore, as shown in Fig. 5, H&E staining results revealed that Gla or Gla-MN-treated scars of the rabbit ear were flatter and thinner than that of Control rabbits, especially in rabbit ear scars of the Gla-MN. For the Blank-MN group, no obvious treatment effect was found aginst scar hyperplasia of rabbit ear compared to the Control rabbits. The pathological scar hyperplasia is commonly induced by uncontrolled fibroblast hyperplasia and the excessive deposition of the extracellular matrix (ECM) during the excessive repair after skin injury (Zhang et al., 2022b). Masson staining can reveal the pathological collagen hyperplasia and epidermal thickness of the scar tissues (Yang et al., 2021). As shown in Fig. 5, Masson staining results showed that a large number of collagen fibers observed in scar tissues of the Control rabbit ear, and both of the treatments with Gla or Gla-MN can alleviate the pathological collagen fibers compared to that of Control rabbits. Importantly, our results also suggested that Gla-MN had a better improving effects against the collagen hyperplasia in scar of rabbit ear than that of Gla treatment (Fig. 5), and similarly, our results also revealed that the blank delivery system carrier had no effect on collagen hyperplasia in scar of rabbit ear (Fig. 5).

3.6. Results of the western blotting assays

In our previous study, we have reported that Gla possessed a therapeutic effects against keloid through inducing the fibroblasts' apoptosis via regulating PI3K/Akt and TGF-β1/SMAD signaling pathways (Zhang et al., 2022b). Consequently, we determined the regulating role of the Gla-MN on pro-apoptotic proteins using western blotting assays. Accumulating evidence has indicated that during the repair process after skin injury, uncontrolled hyperplasia and insufficient apoptosis of the fibroblasts might be one of the leading cause for developing of keloid (Zhang et al., 2022b). Apoptosis, the most important programmed cell death way (PCD), is a physiological cell suicide process (Xu et al., 2024). Nowadays, it's also reported that induction of apoptosis in fibroblasts would be a feasible way for treating scar hyperplasia. Caspase-3, Bax and Bcl-2 are the marker proteins of the cell apoptosis way, in particluarly caspase-3 is a molecular signature for the cells undergoing apoptosis. Caspase-3 and Bax are the pro-apoptotic proteins for cells, whereas Bcl-2 is the anti-apoptotic proteins which has the function to directly bind and suppress the pro-apoptotic proteins' activities (Wang et al., 2024; Zhang et al., 2017b). As can be seen from the Fig. 6, compared to the Control group, both the Gla- ($p < 0.05$) and Gla-MN treatment ($p < 0.01$) can upregulate the pro-apoptotic proteins of cleaved (C)-caspase-3, and the results also revealed that Gla-MN treatment had a higher up-regulating effect on C-caspase-3 than that of Gla treatment. Furthermore, both of the Gla- ($p < 0.05$) and Gla-MN treatment ($p < 0.01$) increased the ratio of Bax/Bcl-2 compared to the Control rabbit, and it seems that Gla-MN treatment had a higher ratio of Bax/Bcl-2 than that of Gla. All these results mentioned above indicated that Gla-MN had a stronger induction of apoptosis in fibroblasts than that of Gla (Fig. 6 A-C).

PI3K/Akt pathway is involved in cell proliferation and

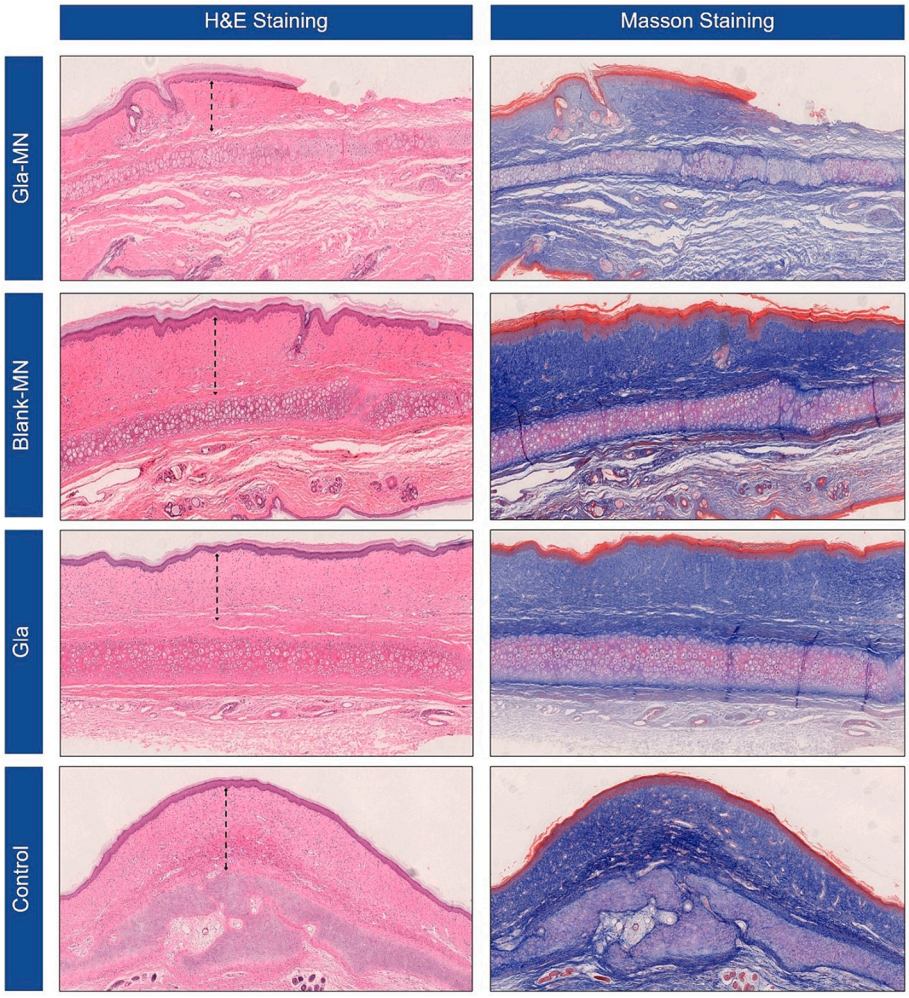

Fig. 5. H&E and Masson straining of hyperplastic scar treated by Gla and Gla-MN on hyperplastic scar rabbit model.

differentiation (Li et al., 2023; Qian et al., 2024), and activated PI3K/Akt pathway would be beneficial for the proliferation and anti-opoptosis of fibroblasts, thus inhibiting the PI3K/Akt pathway might be a feasible way for suppressing scar hyperplasia via induction of apoptosis. For the PI3K/Akt signaling, phosphorylated PI3K and Akt proteins are the activated state. In our present study, we found that Gla- and Gla-MN treatment can inhibit the phosphorylation of PI3K/Akt signaling compared to the Control rabbits ($p < 0.05$), however the results indicated Gla-MN treatment had a stronger inhibition of the phosphorylation of PI3K/Akt signaling than Gla (Fig. 6 C-J). Furthermore, the TGF-β1/α-SMA signaling is closely correlated in producing ECM by fibroblasts, including collagen, fibronectin and aminoglycan. Our results revealed that both Gla- and Gla-MN can down-regulate the TGF-β1 and α-SMA compared to the Control rabbit, and it's intrestingly that Gla-MN treatment had a stronger down-regulating effects on the TGF-β1 and α-SMA than that of Gla (Fig. 6 K-M).

4. Conclusion

In conclusion, the obtained results suggested that dissolving microneedles are a promising transdermal drug delivery modality for assisting drugs to act efficiently across the skin barrier. However, dissolving microneedles use water-soluble materials as the tip, and improving their hardness and skin penetration ability remains a major challenge. In the present study, Gla-MN was successfully prepared by the vacuum filling method with using 10% HA as tip material, which had good hardness and penetration performance. In addition, the backing material was selected as 5% PVA-1799, which had good anti-wrinkle and shrinkage properties, could form smooth and complete microneedle arrays, and also had a high needle formation rate. The drug loading of Gla-MN in this study was about 44 μg/microneedle, which could achieve an effective dose for the treatment of keloids. In addition, the size and shape of the microneedle mold can be adjusted according to the actual application, which can meet a variety of drug loading capacity requirements. The in vitro accumulated drug release rate was approximately 76.9%, which was a vast improvement over normal skin application. Therefore, compared with Gla treatment, Gla-MN treatment had a stronger anti-scar hyperplasia effects in rabbit ear. In addition, Gla-MN treatment also had a higher effect on induction of apoptosis in fibroblasts via showing stronger effect on inhibiting PI3K/Akt and TGF-β1/α-SMA signalings than that of Gla treatment. The reason might be related to the fact that Gla-MN has better skin permeability and higher drug release rate than Gla, which would lead to a higher absorbtion and bioavailability. In conclution, the proposed Gla-MN provides an excellent alternative non-invasive way for clinical treatment of keloid in this study.

Author contributions

Q.R., L.S.H. and W.P. conceived the research and design of all experiments. J.G., Z.T.C., R.H. and Y.H.W. performed the experiment. L.Y.M., L.S.H. and P.S. helped with data analysis. S.G.H. supervised the experiment and reviewed the manuscript thoroughly. J.G. and Z.T.C. wrote the manuscript. W.P. revised the final manuscript.

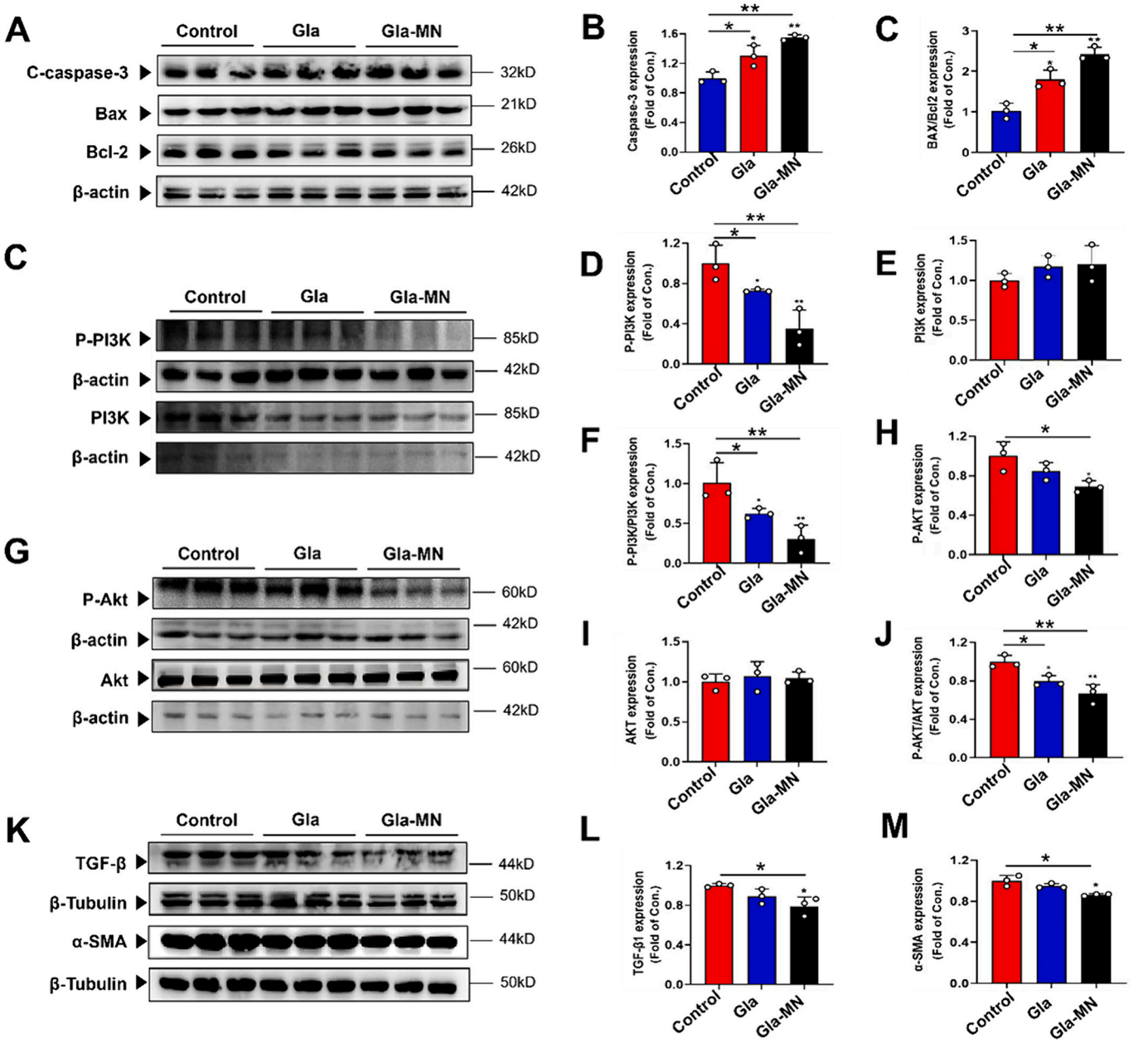

Fig. 6. Western blotting assays. (A)-(C) Expressions of Caspase-3, Bax and Bcl-2; (D)-(G) Expressions of PI3K and p-PI3K; (H)-(K) Expressions of Akt and p-Akt. (L)-(N) Expressions of TGF-β and α-SMA. $*p < 0.05$, $**p < 0.01$, vs. Control.

CRediT authorship contribution statement

Juan Guo: Writing – original draft, Software, Investigation, Formal analysis, Data curation. **Zhongtang Chen:** Writing – original draft, Investigation, Formal analysis, Data curation. **Rong Huang:** Visualization, Investigation, Data curation. **Dandan Tang:** Formal analysis, Investigation, Methodology. **Yuhuan Wang:** Validation, Investigation, Data curation. **Pan Song:** Software, Data curation. **Liangyu Mei:** Software, Data curation. **Shuguang Hou:** Visualization, Software. **Wei Peng:** Investigation, Supervision, Visualization. **Lisha He:** Writing – review & editing, Visualization, Methodology, Conceptualization. **Qiang Ren:** Writing – review & editing, Visualization, Validation, Methodology, Funding acquisition, Conceptualization.

Declaration of competing interest

All the listed authors have read and approved the submitted manuscript, and the authors declare no conflict of interest.

Data availability

Data will be made available on request.

Acknowledgments

This work was supported by the Innovation and Entrepreneurship Projects for College Students of the Science and Technology Park of Chengdu Univerisity of Traditional Chinese Medicine (No. KJYYB2401) and "Xinglin Scholars" discipline talent research promotion project of the Chengdu University of Traditional Chinese Medicine (No. YYZX2021003).

Appendix A. Supplementary data

Supplementary data to this article can be found online at https://doi.org/10.1016/j.ijpx.2024.100267.

References

Ahn, G.R., Jang, Y.N., Lee, S.Y., Kim, W.J., Han, H.S., Yoo, K.H., Bae, T.H., Ban, J.S., Seok, J., Kim, B.J., 2023. Full-thickness skin rejuvenation by a novel dual-length microneedle radiofrequency device: a proof-of-concept study using human skin. Lasers Surg. Med. 55 (8), 758–768.

Chen, Z.A., Gao, Z., Xia, L.L., Wang, X.Q., Lu, L.M., Wu, X.L., 2021. Dysregulation of DPP4-CXCL12 balance by TGF-β1/SMAD pathway promotes CXCR4^{+} inflammatory cell infiltration in keloid scars. J. Inflamm. Res. 144169–144180.

Chen, Z., Liu, X., Jiang, Z., Wu, H., Yang, T., Peng, L., Wu, L., Luo, Z., Zhang, M., Su, J., Tang, Y., Li, J., Xie, Y., Shan, H., Lin, Q., Wang, X., Chen, X., Peng, H., Zhao, S., Chen, Z., 2024. Innovation 5 (3), 100621.

Cheng, Z.T., Lin, H., Wang, Z., Yang, X.Y., Zhang, M., Liu, X.C., Wang, B.J., Wu, Z.F., Chen, D.Q., 2020. Preparation and characterization of dissolving hyaluronic acid composite microneedles loaded micelles for delivery of curcumin. Drug Deliv. Transl. Res. 10 (5), 1520–1530.

Fang, F.J., Huang, R.L., Zheng, Y.C., Liu, M., Huo, R., 2016. Bone marrow derived mesenchymal stem cells inhibit the proliferative and profibrotic phenotype of hypertrophic scar fibroblasts and keloid fibroblasts through paracrine signaling. J. Dermatol. Sci. 83 (2), 95–105.

Ghadiri, S.J., Kloczko, E., Flohr, C., 2022. Topical treatments in the management of keloids and hypertrophic scars: a critically appraised topic. Br. J. Dermatol. 187 (6), 855–856.

Hespeler, D., Kaltenbach, J., Pyo, S.M., 2019. Glabridin smartPearls - Silica selection, production, amorphous stability and enhanced solubility. Int. J. Pharmaceut. 561228–561235.

Hong, J.Y., Ko, E.J., Choi, S.Y., Li, K., Kim, A.R., Park, J.O., Kim, B.J., 2018. Efficacy and safety of a novel, soluble microneedle patch for the improvement of facial wrinkle. J. Cosmet. Dermatol. 17 (2), 235–241.

Jamaledin, R., Yiu, C.K.Y., Zare, E.N., Niu, L.N., Vecchione, R., Chen, G.J., Gu, Z., Tay, F. R., Makvandi, P., 2020. Advances in antimicrobial microneedle patches for combating infections. Adv. Mater. 32 (33), 29.

Jiang, Z.Y., Liao, X.C., Liu, M.Z., Fu, Z.H., Min, D.H., Guo, G.H., 2020. The safety and efficacy of intralesional verapamil versus intralesional triamcinolone acetonide for keloids and hypertrophic scars: a systematic review and meta-analysis. Adv. Skin Wound Care 33 (4), 7.

Kim, Y.C., Park, J.H., Prausnitz, M.R., 2012. Microneedles for drug and vaccine delivery. Adv. Drug Deliv. Rev. 64 (14), 1547–1568.

Knopf-Marques, H., Pravda, M., Wolfova, L., Velebny, V., Schaaf, P., Vrana, N.E., Lavalle, P., 2016. Hyaluronic acid and its derivatives in coating and delivery systems: applications in tissue engineering, regenerative medicine and immunomodulation. Adv. Healthc. Mater. 5 (22), 2841–2855.

Li, M.Y., Tang, D.D., Xu, R.C., Zhang, S.R., Chen, Y., Peng, W., 2023. Uncovering quality markers of Yiqi-Tongluo capsule against myocardial ischemia and optimization of its extraction process. J. Chromatogr. B 123012.

Limandjaja, G.C., Belien, J.M., Scheper, R.J., Niessen, F.B., Gibbs, S., 2020. Hypertrophic and keloid scars fail to progress from the CD34^{-} /α-smooth muscle actin (α-SMA)$^{+}$ immature scar phenotype and show gradient differences in α-SMA and p16 expression. Br J. Dermatol. 182 (4), 974–986.

Lu, Y.J., Cheng, L.S., Ren, L., Chen, D.Q., Guan, S.M., Zhu, S.Y., Xu, X., Zhang, B., Tang, M.H., Zhang, C.J., Ai, Y., Zhang, L.Y., He, T.G., 2024. Therapeutic alleviation and mechanism of glabridin liposome on histamine-induced atopic dermatitis. Pharmacogn. Mag. 10.

Luan, Y., Liu, Y., Liu, C., Lin, Q., He, F., Dong, X., Xiao, Z., 2016. Serum miRNAs Signature Plays an Important Role in Keloid Disease. Curr. Mol. Med. 16 (5), 504–514.

Ning, X.Y., Wiraja, C., Lio, D.C.S., Xu, C.J., 2020. A double-layered microneedle platform fabricated through frozen spray-coating. Adv. Healthc. Mater. 9 (10), 9.

Peng, W., He, C.X., Li, R.L., Qian, D., Wang, L.Y., Zhang, Q., Wu, C.J., 2024. Zanthoxylum bungeanum amides ameliorates nonalcoholic fatty liver via regulating gut microbiota and activating AMPK/Nrf2 signaling. J. Ethnopharmacol. 31815.

Qian, D., Zhang, Q., He, C.X., Guo, J., Huang, X.T., Zhao, J., Zhang, H., Xu, C., Peng, W., 2024. Hai-Honghua medicinal liquor is a reliable remedy for fracture by promotion of osteogenic differentiation via activation of PI3K/Akt pathway. J. Ethnopharmacol. 330, 118234.

Ronnander, P., Simon, L., Spilgies, H., Koch, A., Scherr, S., 2018. Dissolving polyvinylpyrrolidone-based microneedle systems for in - vitro delivery of sumatriptan succinate. Eur. J. Pharm. Sci. 11484–11492.

Sabbagh, F., Saha, P., Kim, B.S., 2023. Transdermal delivery of Catechin using dissolving poly(vinyl alcohol)-based microneedles: effect of microneedle composition on drug release. ACS Appl. Polym. Mater. 5 (11), 8919–8928.

Sartawi, Z., Blackshields, C., Faisal, W., 2022. Dissolving microneedles: applications and growing therapeutic potential. J. Control. Release 348186–348205.

Simmler, C., Pauli, G.F., Chen, S.N., 2013. Phytochemistry and biological properties of glabridin. Fitoterapia 90160–90184.

Srivastava, R.K., Wang, Y., Khan, J., Muzaffar, S., Lee, M.B., Weng, Z.P., Croutch, C., Agarwal, A., Deshane, J., Athar, M., 2022. Role of hair follicles in the pathogenesis of arsenical-induced cutaneous damage. Ann. N. Y. Acad. Sci. 1515 (1), 168–183.

Viswanathan, V., Mukne, A.P., 2016. Development and validation of HPLC and HPTLC methods for estimation of Glabridin in extracts of *Glycyrrhiza glabra*. J. AOAC Int. 99 (2), 374–379.

Wang, Y., Ma, F.S., Wang, Y.N., Xiu, X.L., Liu, Y., Song, W.M., Hu, X.X., 2022. Skin models and its related evaluation of microneedle puncture performance. Prog. Biochem. Biophys. 49 (8), 1406–1421.

Wang, Z.Z., Yi, T.S., He, Y.Y., Zhou, Q., Chen, B., 2024. *Acalypha australis* L. extract inhibits B16 melanoma cell metastasis through PI3K/AKT signaling pathway. Integ Med. Discov 8, e24002.

Ward, R.E., Sklar, L.R., Eisen, D.B., 2019. Surgical and Noninvasive Modalities for Scar Revision. Dermatol. Clin. 37 (3), 375–386.

Wei, S.S., Yang, M., Chen, X., Wang, Q.R., Cui, Y.J., 2015. Simultaneous determination and assignment of 13 major flavonoids and glycyrrhizic acid in licorices by HPLC-DAD and Orbirap mass spectrometry analyses. Chin. J. Nat. Med. 13 (3), 232–240.

Xing, M.Z., Ma, Y.N., Wei, X.C., Chen, C., Peng, X.L., Ma, Y.X., Liang, B.W., Gao, Y.H., Wu, J.B., 2023. Preparation and evaluation of auxiliary permeable microneedle patch composed of polyvinyl alcohol and eudragit NM30D aqueous dispersion. Pharmaceutics 15 (7), 17.

Xu, L., Zhou, Y., Ma, R., Guo, X., Chen, H., Fan, L., Wang, X., 2024. The andrographolide derivative, AND7, AND TRAIL combination attenuates acute lymphoblastic leukemia through P53-regulated ROS accumulation. Acta Materia Medica 3 (2).

Yan, C.X., Xing, M.Z., Zhang, S.H., Gao, Y.H., 2023. Clinical development and evaluation of a multi-component dissolving microneedle patch for skin pigmentation disorders. Polymers 15 (15), 15.

Yang, B., Dong, Y., Shen, Y., Hou, A., Quan, G., Pan, X., Wu, C., 2021. Bilayer dissolving microneedle array containing 5-fluorouracil and triamcinolone with biphasic release profile for hypertrophic scar therapy. Bioact Mater 6 (8), 2400–2411.

Zhan, Y., Xu, X., Luo, X., Liu, R., Lin, Y., Zhao, P., Shi, J., 2023. Preparation of tanshinone IIA self-soluble microneedles and its inhibition on proliferation of human skin fibroblasts. Chin Herb Med. 15 (2), 251–262.

Zhang, C., Luo, S.Q., Zhang, Z.W., Niu, Y.L., Zhang, W.P., 2017a. Evaluation of Glabridin loaded nanostructure lipid carriers. J. Taiwan Inst. Chem. Eng. 71338–71343.

Zhang, M.Z., Dong, X.H., Guan, E.L., Si, L.B., Zhuge, R.Q., Zhao, P.X., Zhang, X., Liu, M. Y., Adzavon, Y.M., Long, X., Qi, Z., Wang, X.J., 2017b. A comparison of apoptosis levels in keloid tissue, physiological scars and normal skin. Am. J. Transl. Res. 9 (12), 5548–5557.

Zhang, T., Wang, X.F., Wang, Z.C., Lou, D., Fang, Q.Q., Hu, Y.Y., Zhao, W.Y., Zhang, L.Y., Wu, L.H., Tan, W.Q., 2020. Current potential therapeutic strategies targeting the TGF-β/Smad signaling pathway to attenuate keloid and hypertrophic scar formation. Biomed. Pharmacother. 12912.

Zhang, X.X., Chen, G.P., Fu, X., Wang, Y.T., Zhao, Y.J., 2021. Magneto-responsive microneedle robots for intestinal macromolecule delivery. Adv. Mater. 33 (44), 10.

Zhang, N., Xue, L.P., Younas, A., Liu, F.F., Sun, J.H., Dong, Z.L., Zhao, Y.X., 2022a. Co-delivery of triamcinolone acetonide and verapamil for synergistic treatment of hypertrophic scars via carboxymethyl chitosan and *Bletilla striata* polysaccharide-based microneedles. Carbohydr. Polym. 28411.

Zhang, Q., Qian, D., Tang, D.D., Liu, J., Wang, L.Y., Chen, W.W., Wu, C.J., Peng, W., 2022b. Glabridin from *Glycyrrhiza glabra* possesses a Therapeutic Role against Keloid via attenuating PI3K/Akt and transforming growth factor-β1/SMAD signaling pathways. J. Agric. Food Chem. 70 (35), 10782–10793.

Zhong, C., Zhang, X.F., Sun, Y.F., Shen, Z., Mao, Y.A., Liu, T.Q., Wang, R., Nie, L., Shavandi, A., Yunusov, K.E., Jiang, G.H., 2024. Rizatriptan benzoate-loaded dissolving microneedle patch for management of acute migraine therapy. J. Biomater. Appl. 38 (9), 989–999.